Catalysis Science & Technology

Accepted Manuscript

ROYAL SOCIETY OF CHEMISTRY

www.rsc.org/catalysis

High specific surface area YSZ powders from a supercritical CO_2 process as catalytic supports for NO_x storage-reduction reaction

Michaela Klotz*[a], Willinton Y. Hernández[b], Christian Guizard[a 1], Céline Viazzi [a], Audrey Hertz[c] Frédéric Charton[c], Caroline Tardivat[a] and Philippe Vernoux[b]

[a] Laboratoire de Synthèse et Fonctionnalisation des Céramiques, UMR 3080 Saint Gobain CREE/CNRS, 550 Avenue Alphonse Jauffret, 84306 Cavaillon, France. Fax: +33 432500964; E-mail: michaela.klotz@saint-gobain.com

[b] Université de Lyon, Institut de Recherches sur la Catalyse et l'Environnement de Lyon, UMR5256, CNRS, Université Claude Bernard Lyon 1, 2 avenue Albert Einstein, 69626 Villeurbanne, France.

[c] CEA Marcoule – DEN/DTCD/SPDE/LPSD - Laboratoire des Procédés Supercritiques et de Décontamination, BP17171, F-30207 Bagnols sur Cèze, France.

[1] Present adress : Institut Européen des Membranes, ENSCM-UM2-CNRS UMR5635, Université Montpellier 2, Place Eugène Bataillon, 34095 Montpellier Cedex 5, France

Acknowledgments

This work has been performed under the collaborative research project MATCOS between SEPAREX, the CEA Marcoule and Saint-Gobain CREE, supported by the French Ministry of Industry under Convention number FCE-DGE N°06 2 90 60 91.

ABSTRACT

Nanometric yttria-stabilized-zirconia (3 mol% Yttria, SC-3YSZ) was synthesized using an innovative supercritical carbon dioxide aided sol-gel process and used as a support for NO_x storage catalysts. Wash-coats composed of noble metals (Pt and Rh) dispersed on 3YSZ were deposited inside the porosity of mini-diesel particulate filters. Commercial and SC-3YSZ powders were used as supports independently and mixed. NO_x storage/reduction performances were compared in cycling conditions according to the YSZ support surface area, the washcoat localization inside the DPF and the metallic dispersions. All the results emphasize that the presence of high specific surface area SC-3YSZ inside the DPF improves the NO_x conversion, the N_2 selectivity and the NO_x storage capacity. This enhancement of the catalytic properties was linked with the increase in both the metallic dispersion and the number of storage sites on the catalyst surface.

Key Words

Yttria-stabilized zirconia; NOx storage-reduction; Diesel particulate filters; supercritical CO_2; sol-gel

1. Introduction

In the past decade, vehicle emissions have been reduced substantially as a result of the European emission legislation. However, particularly in urban areas, NO_x levels have difficulty in meeting the European limits regarding air quality (mainly NO_2). It is known that diesel engines are the main source of NO_x emissions in urban zones [1,2]. Therefore, the emission performance of vehicles under urban driving conditions is of increasing importance. The EURO 6 legislation, from 2014, requires extremely low emission levels of NO_x, decreasing from 0.18 g/km (EURO 5 standard) to 0.08 g/km. The challenge is to develop smart catalysts that are able to selectively reduce NO_x into environmentally benign N_2 in a lean-burn exhaust. NO_x storage-reduction (NSR) catalytic technology emerges as a promising solution for removal of NO_x from these engines [3]. NSR catalysts work in cyclic gas-composition conditions. During the first step (lean phase), NSR materials store emitted NO_x as nitrates until the surface reaches the saturation threshold. A pulse of fuel post-injection then triggers the short second step (rich phase), during which the reducing conditions lead to nitrate decomposition and release as well as subsequent NO_x reduction into N_2 and surface regeneration. NSR materials are commonly composed of Pt nanoparticles to activate NO oxidation into NO_2 in the lean phase, a storage basic compound (typically K or Ba) to form nitrates from NO_2, Rh nanoparticles to reduce NO_x into N_2 in the rich phase and an oxide support [4,5]. NSR catalysts can be inserted into the porosity of diesel particulate filters (DPFs), thus strongly decreasing the space required for the after-treatment, making NSC technology attractive for compact cars. However, NSR catalysts must be sulphur- and temperature-resistant and must contain low noble metal loadings to compete with the

urea-SCR technology. In addition, the fuel overconsumption provoked by the fuel post-injection during the rich phases must absolutely be minimized to avoid a fuel penalty.

Recently, we have shown that yttria-stabilized zirconia (YSZ) can be used as a support for NSR catalysts [6]. A remarkable NO_x storage capacity was obtained on Pt/YSZ powdered catalysts. Under cycling conditions, powdered Pt-Rh catalyst exhibited overall NO_x abatement conversion around 75% between 250 and 300 ºC. In addition, quite reproducible and stable NO_x conversions were achieved by using mini-DPFs impregnated with a Pt-Rh/YSZ catalyst in cycling conditions with values of around 50% between 250 and 400 °C. YSZ-based NSR catalysts have shown high thermal resistance and sulphur tolerance. The ability of YSZ to store NO_x was linked with the ionic conductivity of YSZ and the presence of oxygen vacancies on the YSZ surface, which can act as NO_2 adsorption sites [6].

Furthermore, YSZ is able to burn soot particulates without the use of noble metal [7]. This fully justifies the utilization of YSZ in the composition of NSC materials deposited in the porosity of DPFs. Nevertheless, an improvement in the surface area properties of those types of materials would be desirable for their use as catalytic-active supports.

In a recent report, a versatile and robust method for the synthesis of yttria-stabilized tetragonal powders by using a semi-continuous process in supercritical CO_2 was reported [8,9]. This innovative process enables an easy control of the porous texture, morphology, crystalline structure and size distribution of the obtained powders. The features of such material make the utilization of this new methodology for the synthesis of catalysts and/or catalytic supports very attractive.

The present study reports the development of high surface area YSZ-based NSR catalysts. YSZ nanoparticles were prepared via a supercritical carbon dioxide (called SC) aided sol-gel process [8,9] to achieve much higher surface specific areas than those of commercial YSZ powders. Wash-coats composed of noble metals (Pt and Rh) dispersed on YSZ were

deposited inside the porosity of mini-DPFs produced by Saint-Gobain. Commercial and SC YSZ powders were used as supports independently and mixed. NO_x storage/reduction performances were compared in cycling conditions according to the YSZ support surface area, the washcoat localization inside the DPF and the metallic dispersions.

2. Experimental

2.1 Catalyst preparation and characterization

YSZ powders were synthesized using a supercritical carbon dioxide assisted sol-gel process developed at the CEA/LPSD. A detailed description of the reactor and synthesis procedure can be found in [8,9]. The 3 mol% yttria-stabilized zirconia (denoted as SC-3YSZ) nano-powders were synthesized from a sol containing yttrium acetate and zirconium hydroxyacetate, mixed with isopropanol in the presence of nitric acid. This sol was injected in the autoclave containing CO_2 in supercritical condition, following the conditions reported in [9]. At the end of the reaction, the autoclave was vented and the powder recovered. X-ray diffraction patterns were acquired using an X'Pert (PANalytical-Cu Kα radiation) equipped with a HTK2000 high temperature chamber. The powder was dispersed in ethanol and deposited on a Pt strip. Nitrogen adsorption/desorption measurements were performed on a Micromeritics Tristar II 3020 gas sorptometer. The surface area was determined using the Brunauer-Emmett-Teller (BET) method.

Structured catalytic systems (monoliths) were obtained by wash-coating mini-SiC-DPFs produced by Saint-Gobain. The monolithic supports (diameter=1 inch (25 mm), length=2 inches (50 mm)) consist of an SiC structure composed of longitudinal square channels (~ 1.5 x 1.5 mm) open at both sides and separated by thin walls (~ 0.4 mm thick). Five different catalytic systems (Table 1) were prepared using either pure or mixtures between SC-3YSZ and a commercial 3 mol% yttria-stabilized powder (denoted as TZ3Y, from Tosoh). First, a 5

wt% suspension was prepared by dispersion of the powders in DI water. The pH of these suspensions was adjusted to 3 using acetic acid. An ultrasonic bath was used to ensure good dispersion. The YSZ was deposited inside mini-DPFs by contacting the monolith support with the suspension until the whole suspension was drained into the monolith. The samples were dried overnight at 40 °C. After a thermal treatment of the monolith at 400 °C in air for 1 hour, Pt and Rh (0.3% w/w in regard to the as-deposited wash-coat) were deposited in two successive steps using $(NH_3)_2Pt(NO_2)_2$ and $Rh(NO_3)_3$ as precious metal precursors and stabilized by thermal treatment at 500 °C in air for 1 hour. All the DPF samples have an equivalent catalyst loading of around 16 g/L of DPF. The BET surface of the mixtures was estimated assuming a linear variation of the S_{BET} value with the weight fraction of each powder. The values are reported in Table 1.

Scanning electron microscopy (SEM) images were recorded using a Nova NanoSEM 230 from FEI. The dispersion of precious metal particles on the DPF was evidenced by TEM (JEOL 2010 LaB6) analysis; samples were prepared using the replica method.

2.2 Catalytic performance measurements.

The NSR cyclic measurements were performed on the mini DPF-catalytic systems by using a steel bi-compartment reactor as described in ref [6]. All the samples were pre-treated at 600 ºC in the presence of 10% O_2/He (~10 L/h; 2h) and then in pure H_2 (~3.2 L/h; 1h). Constant flows (40 L/h) of lean reaction mix (500 ppm NO/ 1000 ppm C_3H_6 / 6.7% O_2 / 10 % H_2O and He as balance) or rich reaction mix (500 ppm NO/ 1000 ppm C_3H_6 and He as balance) were alternately introduced into the reactor. The cycling experiments with a lean period of 3 min and a rich period of 2 min were performed at 300 ºC. The catalysts were exposed to 12 lean/rich cycles repeated 3 times for each composition. The NO_x conversion for a complete representative cycle was calculated according to the following formula:

% NO_x conversion = 100 x ($NO_{x,in} - NO_{x,out}$)/$NO_{x,in}$ (1).

The global NO_x conversion into N_2 (selectivity of the process) was estimated considering the production of N_2O during a complete cycle:

% NO_x conversion into N_2 = 100 x ($NO_{x,in} - NO_{x,out} - 2 \times N_2O_{out}$) / $NO_{x,in}$ (2).

3. Results and Discussion.

3.1 YSZ powders characterizations

Detailed characterizations of the nano-powders synthesized in supercritical CO_2 can be found in [8,9]. During the wash-coating, precious metal deposition and catalytic tests, thermal treatments up to 600 °C were performed. The crystal structure and specific surface area of the SC-3YSZ nano-powder were therefore checked after a thermal treatment at 600 °C for 10 h, in order to be representative of the coatings in the DPF. The XRD patterns of the 600 °C thermal treated powder can be indexed to yttria-stabilized zirconia. The diffraction peaks are wide, indicating that the crystal size remains nanometric, estimated to be approximately 9 nm from the Scherrer equation.

It was not possible to determine the nature of the crystal phases (between cubic and tetragonal), as shown in the enlarged view around the main diffraction peaks (Figure 1). The structure of the 3 mol% yttria-doped zirconia is usually tetragonal. This was confirmed by XRD after a calcination of the SC-3YSZ powder at 1200°C in air for 10 hours (Figure 1-b).

Due to its nanosized nature, the as-synthesized SC-3YSZ powder exhibits a high specific surface area (SSA) of 170 m²/g. After calcination at 600 ºC for 3 hours, its SSA remains important at 40 m^2/g. Thus, compared to the SSA of TZ3Y material (15 m^2/g; 700 ºC annealing temperature), the use of the SC-3YSZ solid represents a clear improvement.

3.2 YSZ-based mini DPFs characterizations

SEM observations were performed to localize the catalytic wash-coat inside the mini-DPFs (Figure 2 and Figure 3). The commercial TZ3Y-based catalyst (DPF-A) is mainly accumulated on the surface of the channels, whereas the SC-3YSZ based material is predominantly located inside the porous walls (DPF-E). The deposition conditions were identical for all samples. It should be noted that the coating was performed by simple contact of the suspension with the monolith without any specific pressure drop to force the penetration of the coating suspension into the DPFs' porous walls. Therefore, the localization of the YSZ coating should only be linked to the viscosity and the granulometry of the suspension. The surface agglomeration for TZ3Y-based samples may be explained by the different agglomeration states of these powders in the suspension. For the mixed samples between the two YSZ powders, the catalytic material is deposited both on the channel surfaces and inside the porosity. This is particularly marked for the DPF-E sample, for which the catalytic layer seems to be homogeneously distributed everywhere inside the monolith. For low catalyst loading on the channel surfaces, the catalyst seems to be preferentially located at the SiC grain boundaries (see, for instance, Figure 2d). According to the localization of the catalyst inside the DPF, the contact time between the gas reactant and the catalyst surface can vary strongly. The high dispersion of SC-3YSZ powder in the porous wall most probably enhances this contact time in comparison with a TZ3Y layer only located on the channel surfaces.

The metallic particle size distribution in the samples was determined by using TEM on the spent catalysts. The catalytic wash-coat was scratched off the SiC substrate. Figures 4 and 5 were obtained after dissolution of the YSZ support using the replica method. For the DPF-A catalyst (Figure 4), Pt and/or Rh nanoparticles are well dispersed and present a particle size distribution range from 1 to 7 nm, centred above 3 nm. Unfortunately, the lattice parameters of these metallic phases are very close and it was not possible to distinguish Pt particles from

Rh ones, even by using an electron diffraction technique or microprobe. The DPF-E sample (Figure 5) exhibits a narrower distribution in size, centred at 2.5 nm. Nevertheless, some particles with sizes between 6 and 10 nm were also observed on the DPF-E catalyst. Such "bigger" particles constitute only a small fraction of the total particles analysed (frequency ≤ 2%).

3.3 NO_x storage/reduction (NSR) cyclic performance measurements

Figure 6 depicts a characteristic NO_x profile achieved during an overall cycle. During the lean phase, part of the NO_x is stored on the catalyst (St_{NOx}), whereas another part reacts with the hydrocarbon (propene) to produce N_2 and N_2O via the selective catalytic reduction (SCR) of NO_x with propene (SCR conversion). In about 50 seconds, the NO_x level reaches a plateau which corresponds to the SCR conversion. Parameters have been used to compare the catalytic performances of the different samples: duration (in seconds) at the beginning of the lean phase profile where the NO_x uptake by the catalyst is complete (t_{100}); total NO_x conversion during one complete lean/rich cycle (C_{NOx}); conversion of NO_x into N_2 for the same cycle, which represents the selectivity of the process (selectivity to N_2); the NO_x plateau concentration at the end of the lean phase, related with the SCR activity of the catalysts; conversion of propane during the rich phase (C_{C3H6}); and finally, the amount of NO_x stored during the lean phase, normalized per gram of catalyst (St_{NOx}) (see Figure 6).

Figure 7 displays the evolutions of the NO_x concentration in the outlet feed as a function of time, between the second and fourth lean/rich cycles, performed at 300 ºC. At the beginning of lean phases, the NO_x level drops to essentially zero, showing a complete uptake of NO_x by the catalyst, except for the system composed only of the commercial support (DPF-A). This complete uptake was sustained for about 100s seconds, and then the NO_x level started gradually increasing with time, reaching a stable value, related to the catalytic properties of

the material's SCR [10,13]. The obtained profiles are very similar to those reported for the NO_x-trap cycling process on $Pt/Ba/Al_2O_3$ catalysts [11,12]. In the present case, the YSZ acts as a NO_x trap, as already demonstrated for Pt/Rh-YSZ supported catalyst, working under similar reaction conditions [6]. In general, the efficiency of the NSR process on the evaluated systems depends on the loading of the high surface area material (SC-3YSZ). DPF-A shows the lowest NO_x storage/reduction capacity, followed by DPF-B, and then very similar profiles were obtained for DPF-C, DPF-D and DPF-E systems. Table 2 summarizes the principal results obtained for the studied systems. All parameters were calculated for cycle No. 5 but are representative of all 12 cycles.

An increase in SC-3YSZ fraction provokes the enhancement of the catalytic performance (Table 2). The NO_x conversion increases from 49 to 72 % between DPF-A and DPF-E. The DPF-A system did not show any total uptake of NO_x during the lean phase. On the other hand, the other materials achieved and maintained a total NO_x storage for several seconds. The t_{100} parameter was increased by ~10 seconds between the DPF-B and DPF-C systems and remained comparable for DPF-D and DPF-E, reaching 56 s. Actually, if one compares the amounts of NO_x stored during the lean period, the values of DPF-D and DPF-E are almost twice that of DPF-A.

The NO_x storage capacity (St_{NOx}) of the DPF-A is around 15 μmol/g_{cat} at 300°C. This value is lower than that previously reported on commercial 8YSZ from TOSOH (34 μmol/g_{cat} at 250 ºC, from reference [6]). Although in both cases the stored NO_x was estimated under different reaction conditions, one can expect lower NO_x storage capacity on 3YSZ oxide used here, due to its lower oxygen vacancy concentration (lower Y_2O_3 doping level in comparison to 8YSZ). When the surface area is promoted by increasing the mass fraction of SC-3YSZ in the catalyst formulation, the total amount of the stored NO_x comes very close to that observed on 8YSZ [6]. Therefore, a lower oxygen vacancy concentration on the commercial 3YSZ oxide

is compensated by an improved SSA of the material synthesized under supercritical conditions.

A remarkable increment in the N_2 selectivity was observed for DPF-D and E (Table 2), i.e. mainly composed of SC-3YSZ. The N_2 selectivity increases from 33% to 59%. This result means that the selective NO_x conversion into N_2 is improved by the high SSA 3YSZ material.

In addition, the NO_x concentration plateau achieved at the end of the lean phase was decreased with the increase of the SC-3YSZ material present in the DPF's porosity (Table 2). The observed NO_x concentration plateau follows the trend: DPF-A < DPF-B < DPF-C ≈ DPF-D ≈ DPF-E. This behaviour must be related with an improved SCR activity of the systems by enhancing their metallic dispersion and/or surface area properties [13].

All these results emphasize that the SSA enhancement of the 3YSZ support improves the NO_x conversion, the N_2 selectivity and the NO_x storage capacity of the wash-coat. This enhancement of catalytic properties is probably linked with the increase in the metallic dispersion, observed by TEM (Figure 5), and the number of storage sites on the catalyst surface. This confirms the key role of surface oxygen vacancies in the NO_x storage process. The characteristics of the catalytic wash-coats inside the mini-DPFs as a function of the SC-3YSZ mass fraction, observed by SEM analysis, should also present an incidence in the catalytic properties of the analysed systems. As discussed before, the commercial YSZ-based catalyst (DPF-A) is mainly accumulated on the surface of the channels while the SC-3YSZ based material is predominantly present inside the porous walls (DPF-E). For DPF-C, DPF-D and DPF-E, the good repartition in the porous walls can improve the contact surface of the system with the gas phase and consequently, the catalytic performances. Therefore, both the better distribution inside the monolith and the highest SSA can explain these improved catalytic properties.

The N_2 selectivity enhancement can also depend on the number, accessibility and nature of the active places on the catalyst surface where the N_2O decomposition can be improved. Centi et al. have reported a significant promotion of Rh-supported catalysts on the N_2O decomposition when M^{3+} doped zirconia was used as a support [13,14]. For these authors, the stabilization of oxygen vacancies at the Rh-doped zirconia interface enhances the effective removal of ad-atoms (formed by N_2O dissociation) from the Rh surface (rate-limiting step of the reaction) [14], and leads to a parallel enhancement of the rate of N_2O dissociation. SC-3YSZ, which combines a partial substitution of Zr^{4+} cations by Y^{3+} ones with a high SSA, may also have a high concentration of surface oxygen vacancies which can explain high values of the N_2 selectivity for DPF-D and E (Table 2).

Propylene was chosen as the reductant because it has a relatively low light-off temperature and clean burn characteristics [15]. From the analysis of the CO_2 profile, it is possible to evaluate the oxidation properties of the catalytic systems during the lean reaction conditions and the ability of the propylene as reducing agent when the flow reaction switches to the rich phase.

Figure 8 shows the CO_2 concentration profiles at 300°C as a function of the time from the second to the fourth lean/rich cycles, obtained during the NO_x-trap reaction.

The CO_2 profiles can be described as follows: at the beginning of the lean phase, a sharp and intense CO_2 peak evolution was observed, due to the oxidation of carbon deposited during the previous rich phase via the Boudouard reaction, as already observed in reference [6] at 250°C. Then, the amount of CO_2 produced in the course of the lean phase corresponds to the propylene oxidation. Discarding the DPF-A system, the propylene conversion into CO_2 achieved for all the other systems was above 95 % (Table 2, C_{C3H6} column). The low oxidation capacity observed on DPF-A (48 %) confirms its low metallic dispersion.

When the flow was switched to rich phase composition, the CO_2 concentration rapidly decreased due to the absence of oxygen. At the end of the rich phase, the CO_2 production can be principally attributed to the SCR process of NO with C_3H_6, the maximum value of which, considering the fed composition and reaction stoichiometry, would be around 166 ppm. The corresponding CO_2 concentration values observed at the end of the rich phase on the studied systems were close to 170 ppm, which fits well with the value expected from the SCR reaction. We have recently evidenced that electrochemical reactions can take place on similar catalytic systems (Pt/Rh / YSZ) and improve the NO_x removal efficiency if the catalysts are deposited in conductive SiC (N-doped SiC) mini-DPFs [16]. Detailed analysis of rich phases has shown an overproduction of CO_2, which was attributed to electrochemical CO oxidation by O^{2-} ions contained in YSZ. In this present study, the SiC-DPFs were non-conductive as non-N doped. Therefore, no CO_2 overproduction was evidenced during rich phases. The coupling of nanosized YSZ supports prepared under supercritical conditions and conductive N-doped SiC DPFs could combine the promoting effects of electrochemical reactions and high surface specific area.

4. Conclusions

Nanosized SC-3YSZ particles were synthesized under supercritical conditions. The properties of these oxide particles, i.e., high surface area, and crystallinity, make them promising materials as catalyst supports. Commercial and SC-3YSZ powders were used, independently and mixed, as catalytic supports. NO_x storage/reduction performances were compared in cycling conditions according to the YSZ support surface specific area, the wash-coat localization inside the DPF and the metallic dispersions. All the results emphasize that the presence of high specific surface area 3YSZ inside the DPF improves the NO_x conversion, the N_2 selectivity and the NO_x storage capacity of the wash-coat. This enhancement of the

catalytic properties was linked with both the increase in the metallic dispersion and the number of storage sites on the catalyst surface. In conclusion, the use of supercritical CO_2 medium for the synthesis of metal oxide catalyst supports can significantly improve the catalytic performance in comparison with conventional supports.

References

[1] U. Adler, *Diesel fuel injection*, Robert Bosch GmbH, 1994
[2] J. Summers, S. Van Houtte, D. Psaras, *Appl. Catal. B*, 1996, **10**, 139
[3] N. Takahashi, H. Shinjoh, T. Iijima, T. Suzuki, K. Yamazaki, K. Yokota, H. Suzuki, N. Miyoshi, S. Matsumoto, T. Tanizawa, T. Tanaka, S. Tateishi, K. Kasahara, *Catal. Today*, 1996, **27**, 63
[4] S. Roy, A. Baiker, *Chem. Rev.*, 2009, **109**, 4054
[5] P. Granger, V.I. Parvulescu, *Chem. Rev.*, 2011, **111**, 3155
[6] W.Y. Hernández, A. Hadjar, M. Klotz, J. Leloup, A. Princivalle, C. Tardivat, C. Guizard, P. Vernoux, *Appl. Catal. B*, 2013, **130-131**, 54.
[7] E. Obeid, L. Lizarraga, M.N. Tsampas, A. Cordier, A. Boréave, M.C. Steil, G. Blanchard, K. Pajot, P. Vernoux, *Journal of Catalysis*, 2014, **309**, 87-96
[8] A. Hertz, Y-M. Corre, S. Sarrade, C. Guizard, A. Julbe, J-C. Ruiz, B. Fournel, *J. Eur. Ceram. Soc.*, 2010, **30**, 1691.
[9] A. Hertz, M. Drobek, J.-C. Ruiz, S. Sarrade, C. Guizard, A. Julbe, *Chemical Engineering Journal*, 2013 **228,** 622-630
[10] S.I. Matsumoto, Y. Ikeda, H. Suzuki, M. Ogai, N. Miyoshi, *Appl. Catal. B*, 2000, **25**, 115
[11] W.S. Epling, J.E. Parks, G.C. Campbell, A. Yezerets, N.W. Currier, L.E. Campbell, *Catal. Today*, 2004, **96**, 21
[12] W.S. Epling, A. Yezerets, N.W. Currier, *Appl. Catal. B*, 2007, **74**, 117
[13] G. Centi, G.E. Arena, S. Perathoner, *J. Catal.*, 2003, **216**, 443
[14] G. Centi, L. Dall'Olio, S. Perathoner, *Appl. Catal. A*, 2000, **194-195**, 79
[15] R.L. Muncrief, K.S. Kabin, M.P. Harold, *Aiche Journal*, 2004, **50**, 2526
[16] W.Y. Hernández, A. Hadjar, A. Giroir-Fendler, P. Andy, A. Princivalle, M. Klotz, A. Marouf, C. Guizard, C. Tardivat, C. Viazzi, P. Vernoux, *Catal. Today*, 2015, **241**, 143-150

Figure 1

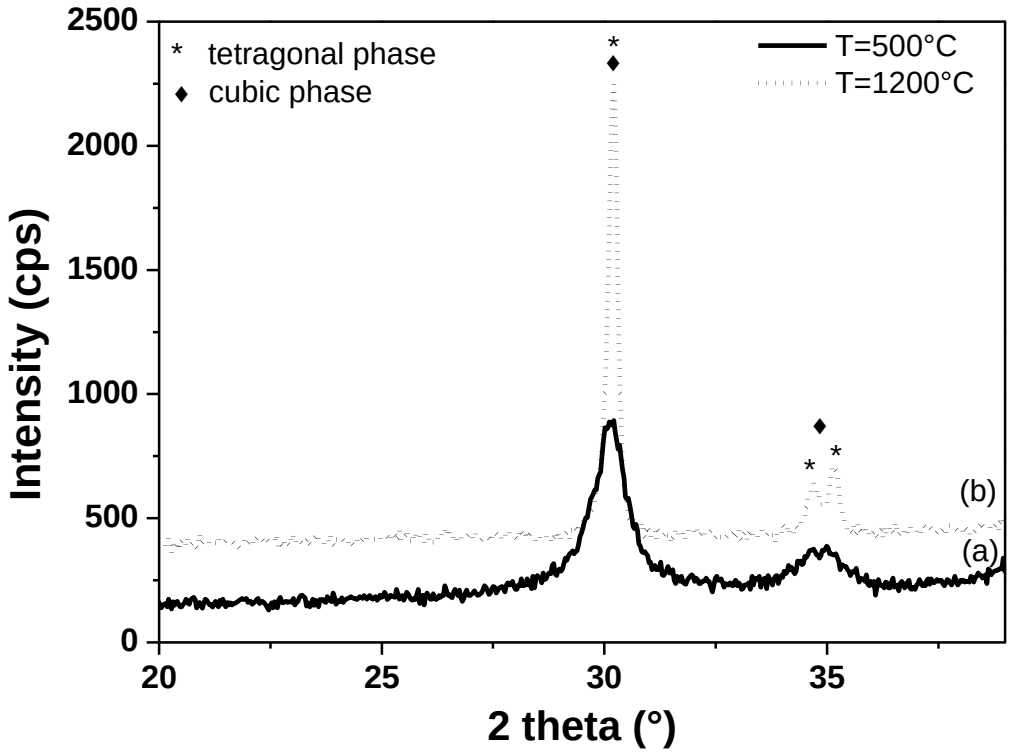

Figure 1: XRD patterns of SC-3YSZ after thermal treatment at 500°C (a) and 1200°C (b).

Figure 2

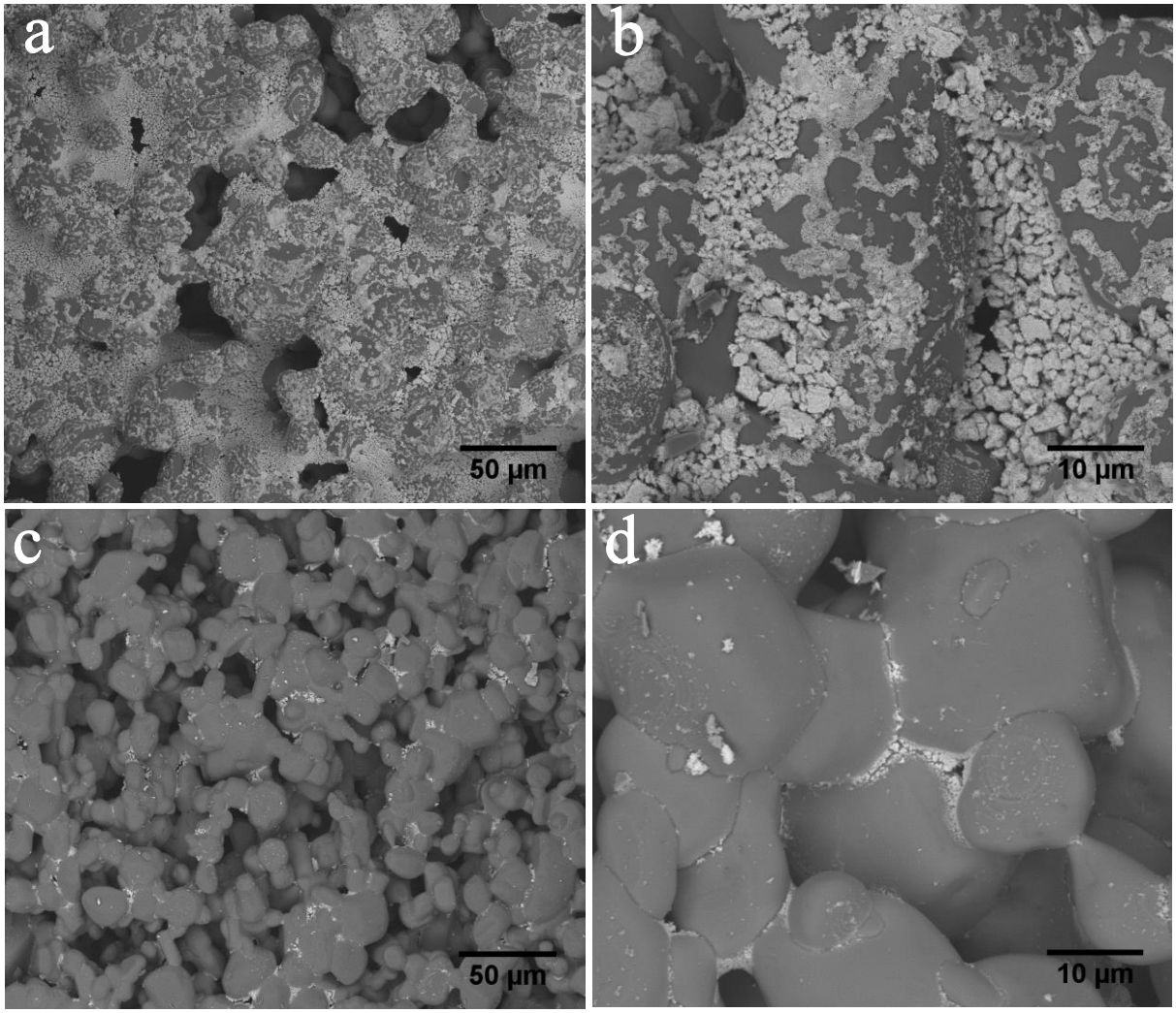

Figure 2: SEM images of the DPF channels surface: (a) and (b) DPF A; (c) and (d) DPF E

Figure 3

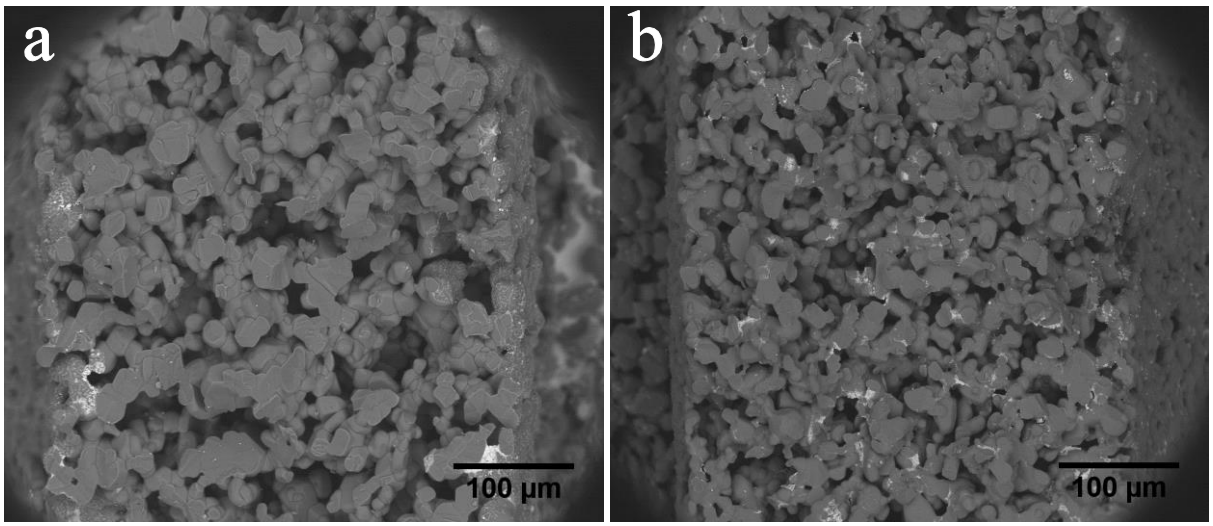

Figure 3. SEM, cross section of DPF porous walls (a) DPF A; (b) DPF E

Figure 4

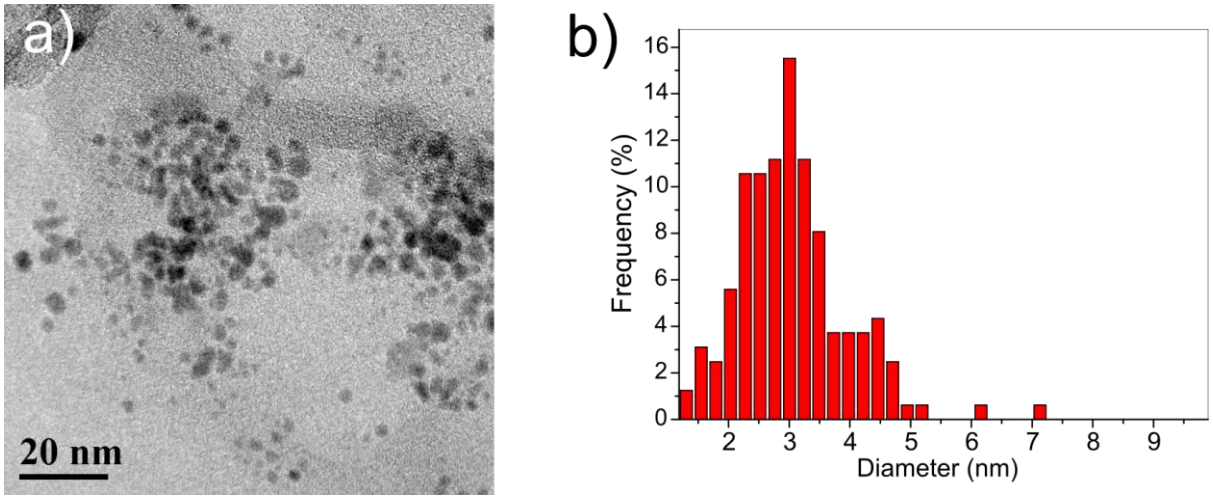

Figure 4 : TEM observations of the catalytic wash-coat deposited on the mini-DPF A. a) typical TEM image of the metallic nanoparticles and b) distribution in size of the metallic nanoparticles (Pt and Rh)

Figure 5

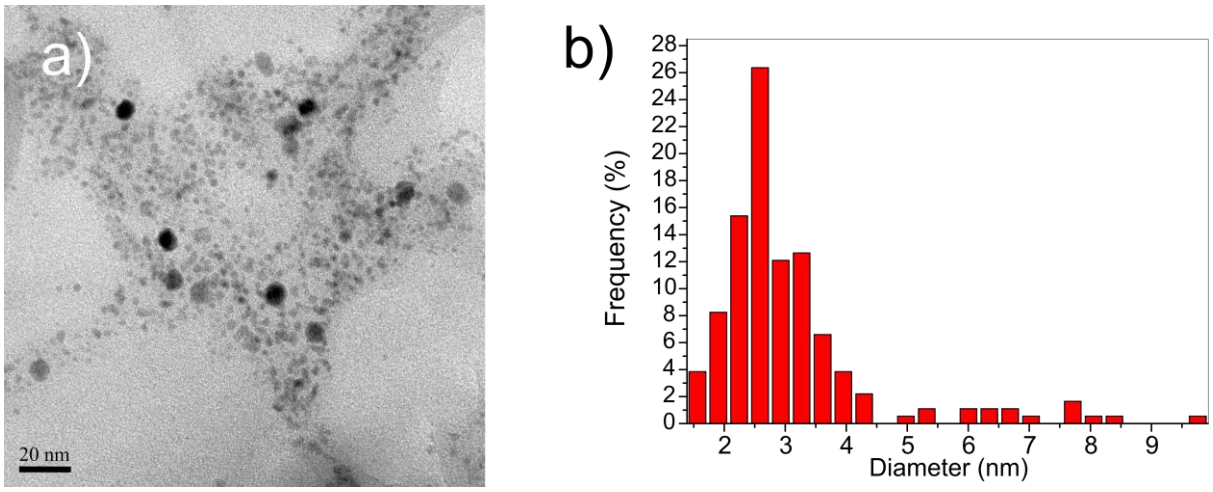

Figure 5. TEM observations of the catalytic wash-coat deposited on the mini-DPF-E. a) typical TEM image of the metallic nanoparticles and b) distribution in size of the metallic nanoparticles (Pt and Rh)

Figure 6

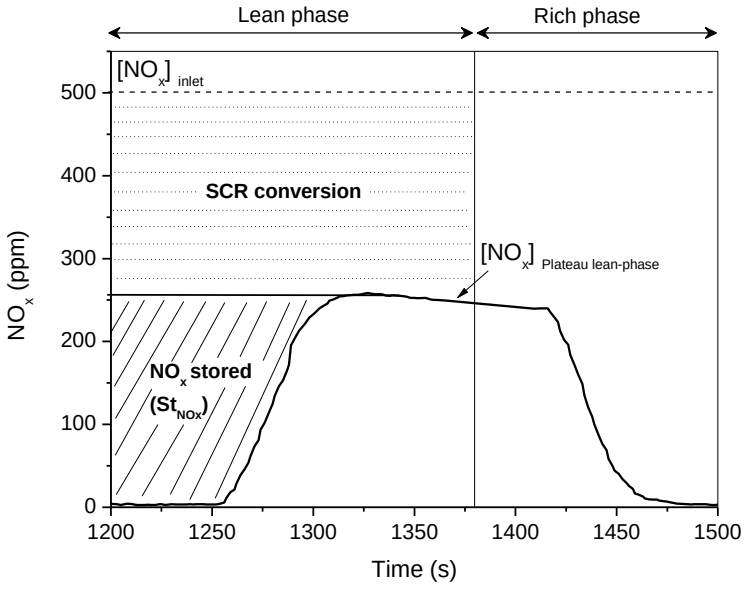

Figure 6. Characteristic NO_x profile obtained for the 5th cycle of the NSR process

Figure 7

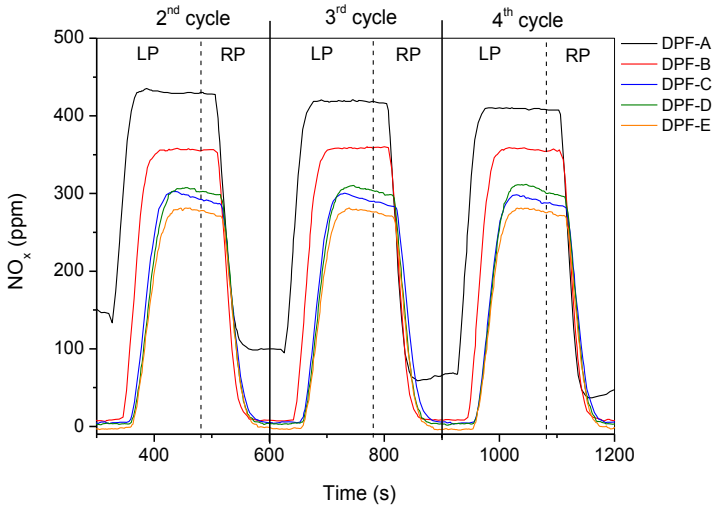

Figure 7: NO_x concentration profiles obtained at 300°C from 2nd to 4th lean/rich cycles.

Figure 8

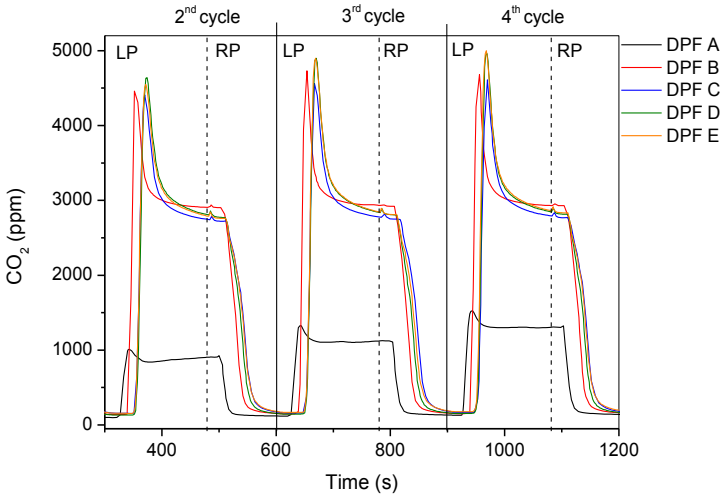

Figure 8: CO_2 concentration profiles obtained from 2nd to 4th lean/rich cycles.

Tables

Table 1. Weight fractions of SC-3YSZ in the as deposited washcoats and theoretical specific surface areas of washcoated powders

Sample	*DPF A*	*DPF B*	*DPF C*	*DPF D*	*DPF E*
$X_{SC\text{-}3YSZ}$	0	0.5	0.6	0.8	1
S_{BET}^{th}	15	27.5	30	35	40

Table 2: Catalytic parameters evaluated on the studied catalytic systems (cycle No. 5) at 300°C.

Monolith	$X_{SC\text{-}3YSZ}$	t_{100} (s)	C_{NOx} (%)	$S_{NOx\ to\ N2}$ (%)	St_{NOx} (µmol/g_{cat})	C_{C3H6} (%)	NO_x plateau lean-phase (ppm)
DPF-A	0	0	49	22	15	48.4	405
DPF-B	0.5	46	62	30	23	96.6	348
DPF-C	0.6	56	69	33	26	93.2	290
DPF-D	0.8	56	69	56	30	95.0	303
DPF-E	1.0	56	72	59	28	95.8	278